

Theoretical Seismology Exam.
2005-2006. M. Campillo and F. Cotton.
3 hours. Lectures notes accepted.

Part 1

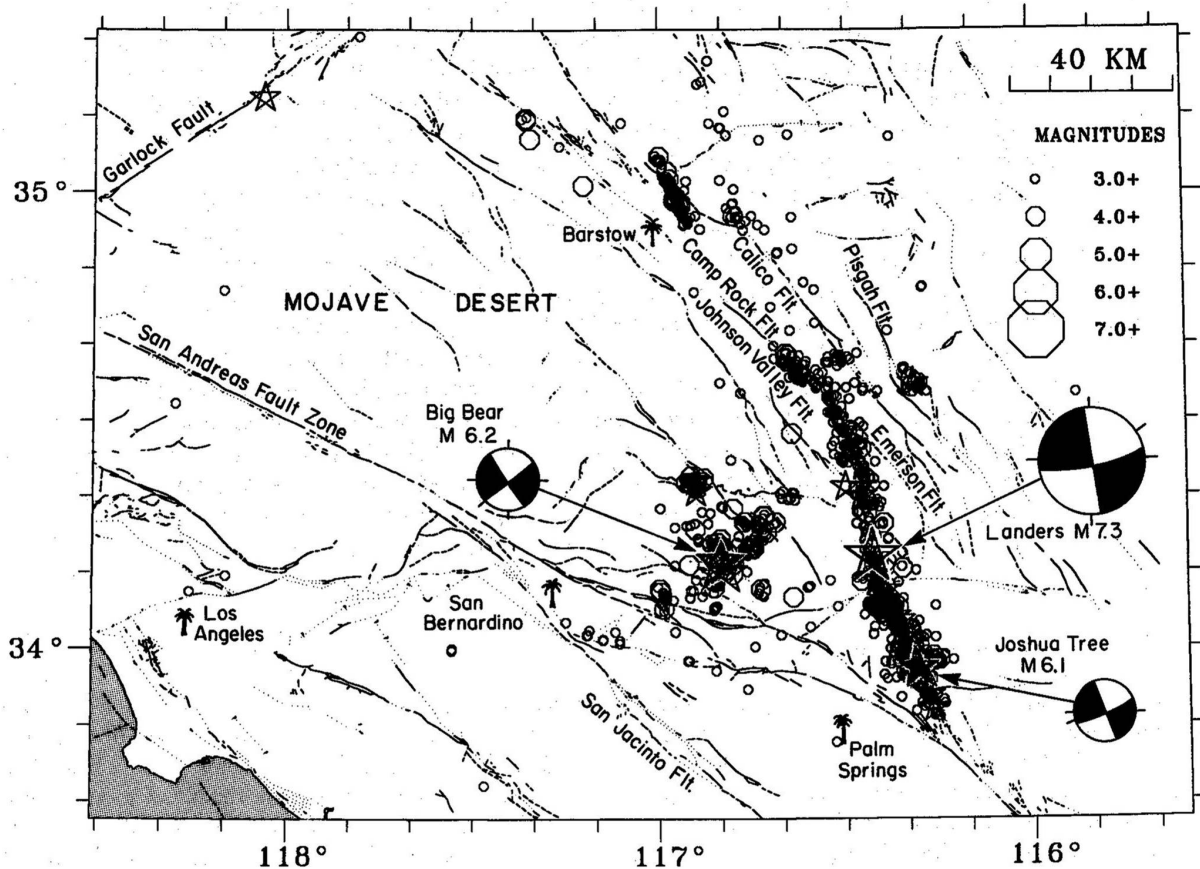


Figure 1. Map of southern California including the eastern California shear zone (Dokka and Travis, 1990), showing major faults from Jennings (1975), and the locations and first-motion focal mechanisms of the 1992 M_w 6.1 Joshua Tree, M_w 7.3 Landers, and M_w 6.2 Big Bear earthquakes and aftershocks of $M \geq 3$. Aftershocks of $M \geq 5$ are shown as stars. Palm trees indicate locations of cities.

Figure 1 shows the focal mechanism of the Landers ($M_w=7.3$) and Joshua Tree ($M_w=6.1$) earthquakes and their aftershocks distributions. Stars indicated the epicentres of the major events.

- 1a. Calculate the Seismic Moment of the Landers and Joshua Tree earthquakes
- 1b. Are these earthquakes strike slip, reverse or normal fault mechanism ?
- 1c. Without any calculation give an estimation of the length and mean slip of the Landers earthquake
- 1d. How many earthquakes of magnitude equal or more than 7.3 do we observe in the world each year ?

Part 2

Model 1
Table 1: Layered Crustal Structure in Southern California

Depth (km)	V _P (km/s)	V _S (km/s)	Density (kg/m ³)	Q _P	Q _S
0.0	5.50	3.20	2800	500	500
4.0	6.30	3.65	2900	500	500
26.0	6.80	3.90	3100	500	500
32.0	8.20	4.70	3200	500	500

Model 2

Depth . km	V _P . km/s	V _S . km/s	Density . Mg/m ³	Q _P	Q _S
0.0	4.1	2.3	2.5	300	300
2.0	5.5	3.2	2.8	500	500
4.0	6.3	3.65	2.9	500	500
26.0	6.8	3.9	3.1	500	500
32.0	8.2	4.7	3.2	500	500

Table 1 presents two falt layers models found in the literature for the crustal structure in southern California. They differ by the presence of a shallow low velocity layer in model 2. We focus in this part on the propagation effects associated with this layer. To simplify we limit our analysis to the case of Love wave. At the first order let consider a single layer over a half space having the properties of the second layer (the case which was treated in the course).

Let consider the harmonic case at frequency f . We consider a plane wave propagating in the shallow layer and contributing to the Love wave. Let us call i the angle of incidence of the plane wave with respect to vertical.

- 2a- Define the phase velocity C in terms of i and the shear wave velocity V_S
- 2b- Give the range of i for which the plane wave can be associated with a Love wave. Identify the lower limit angle and give its numerical value.
- 2c- Demonstrate that a source far below the layer cannot produce a Love wave
- 2d- Explain why the presence of inhomogeneities in the shallow layer can result in the observation of Love waves. In the case when the inhomogeneity consists of a small variation of shear velocity in a known limited volume, does the amplitude of Love wave give an indication on the amplitude of the velocity variation ?
- 2e- We consider again an homogeneous layer over a half space. We remind here the dispersion relation established in the course:

$$\mu(1 - \frac{C^2}{\beta^2})^{1/2} - \mu'(\frac{C^2}{\beta'^2}) - 1)^{1/2} \tan(kh(\frac{C^2}{\beta'^2}) - 1)^{1/2}) = 0$$

Identify and give the values of the parameters you know in the present example.

- 2f Give the limit value of the frequency and the phase velocity associated with the limit $i \rightarrow i_c$ where i_c is the critical angle.

- 2h Same question for $i \rightarrow \frac{\pi}{2}$

Part 3. Directivity effect and slip distribution

Source time function information contained in seismic signals is obscured by propagation and recording effects. To isolate the farfield source time function from propagation and instruments effects, one can deconvolve surface waves (or body waves) of a large event from the surface waves (or body waves) of a moderate-size event. The small event must be near the mainshock and have a similar depth and focal mechanism. An event satisfying these criteria is called an empirical Green Function (EGF) as it constitutes an approximate point source impulse response for a given moment tensor.

Such a deconvolution has been applied by Velasco et al. (1994). The large event is the Landers ($M_w=7.3$) earthquake. The small event (EGF) is the Joshua Tree ($M_w=6.1$) earthquake.

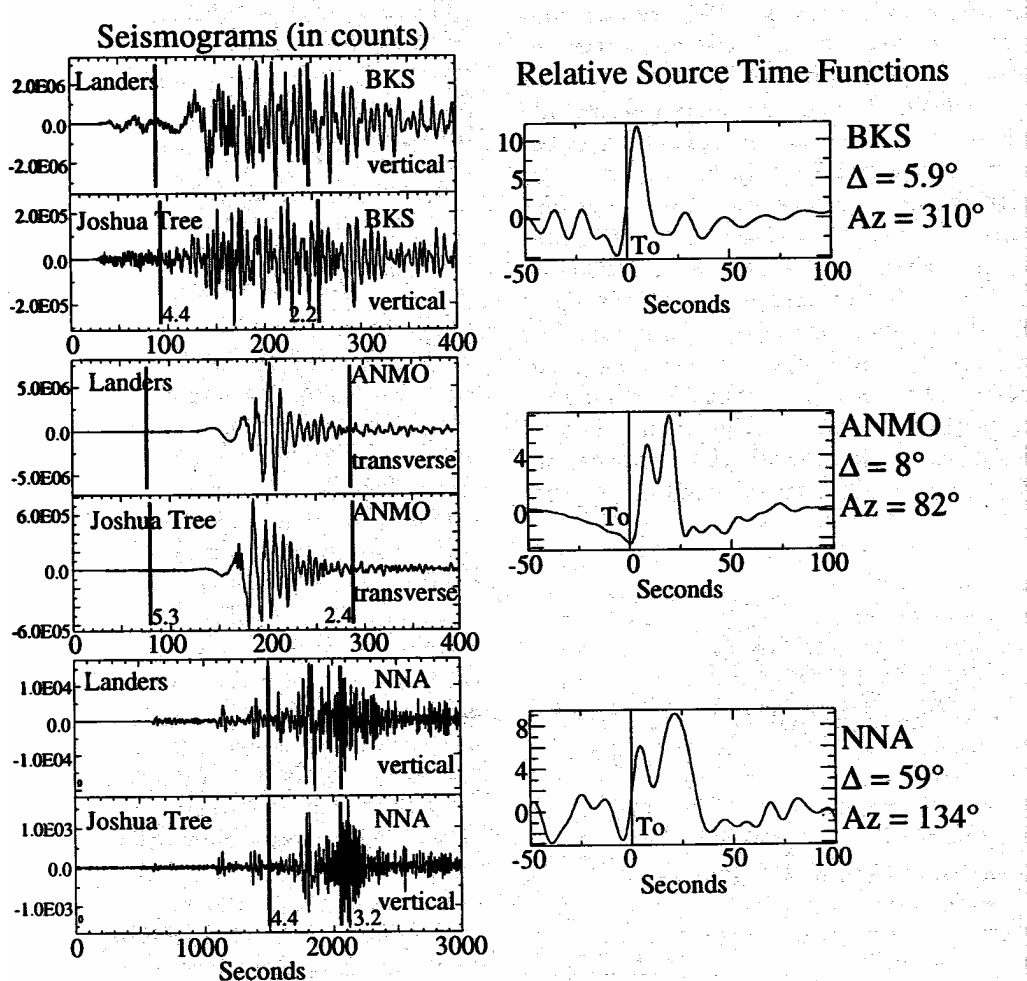


Figure 2. Example of source time function extraction for the deconvolution of surface waves recorded at ANMO, NNA and BKS. Each surface-wave arrival is group velocity windowed (vertical lines in seismogram window). The Joshua Tree ($M_w = 6.2$) earthquake recordings are deconvolved from the Landers ($M_w = 7.3$) earthquake recordings. Each deconvolution gives a relative source time function at each station for the Landers earthquake (right).

The figure 2 shows some source time function extraction $f(t)$ for the deconvolution of surface waves for some teleseismic stations. The station BKS is located north of the Landers earthquake, ANMO is located east of the Landers earthquake (perpendicular to the fault) and NMA located south of the earthquakes.

These source time functions show two pulses for the NMA and ANMO stations and one pulse only for the BKS station. The duration of the source function is larger for the NMA station than for the ANMO station. Velasco et al. explain these complex source times function by directivity effects and by the fact that the earthquake is dominated by two subevents (two regions of high slip separated by a region of lower slip).

In this analysis δt is the measured time difference observed on a station between the onset of the rupture (hypocenter) and the time arrival of the second pulse (second subevent), t_0 is the real time separation between the onset of the rupture and the second subevent and Δ is the distance between the onset of the rupture (hypocenter) and the second subevent.

$$3a. \text{ Show that } \delta t = t_0 - \Gamma \Delta \quad \text{with } \Gamma = \frac{\cos \theta}{c}$$

Γ is a directivity parameter where θ is the azimuth of the station relative to the azimuth of a line connecting the spacial offset between the features and c is the wave velocity which is assumed to be equal to 3.8 km/sec

δt is investigated systematically for stations located at different azimuth from the fault (Figure 3). The preferred fault strike (355°) corresponds to the direction producing the best linear correlation coefficient for (1).

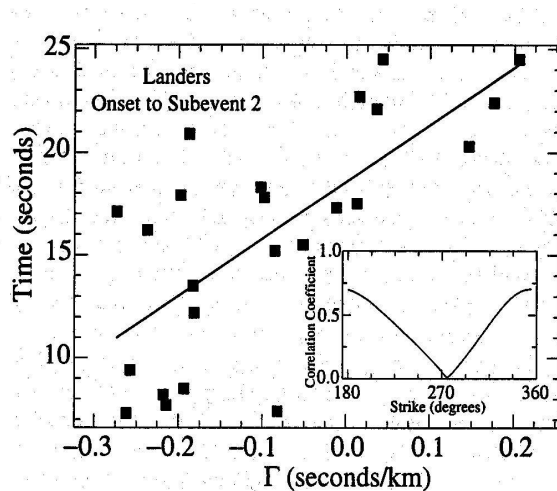


Figure 3 . Directivity analysis of the second subevent relative to the onset of motion of the Landers earthquake. The inset shows the variation of the corresponding linear correlation coefficient as a function of azimuth. The maximum value occurs at a strike of 335° , which is the case shown. Squares correspond to individual observations, the best fitting line is indicated by the solid line.

3b. Which is the distance Δ between the rupture onset and the second subevent ?

3c. Which is the rupture velocity between the onset and the second sub-event ?

We now assume that the entire rupture propagates with constant rupture velocity and that the slip function on each point of the fault is a step function $dD(x,t)/dt=\delta(t)$ where $D(x,t)$ is the slip, x the distance along the strike direction en t the time. $\delta(t)$ represent the dirac function.

The moment rate function is then equal to $\dot{m}(x, t) = m(x) \otimes \delta\left(t - \frac{x}{v_R}\right)$

with $m(x) = \mu W S(x)$ μ is the shear modulus, W the width of the fault and $S(x)$ the slip on the fault along the strike direction.

The source time function $f(t)$ observed at station ANMO perpendicular to the fault can then be written

$$f(t) = \frac{\left(\int_{-\infty}^{\infty} m(x, t) dx\right)}{m_0_{egf}}$$
 where m_0_{egf} is the seismic moment of the Joshua Tree earthquake used as EGF in the deconvolution.

3d. Using the following relationship $\delta(ax + b)) = \frac{1}{|a|} \delta\left(x + \frac{b}{a}\right)$ show that

$$f(t) = \frac{(v_R m(tv_R))}{m_0_{egf}}$$

3e. Using the $f(t)$ observed at the station ANMO deduce the slip profile of the Landers earthquake along the fault.

Part 4. Interpretation of strong motions

A simplified model of the Landers rupture with 2 linear segments is presented in Figure 4. The rupture reaches the upper low velocity layer (dashed line). On each segment the rupture develops in a manner similar to the Haskell model.

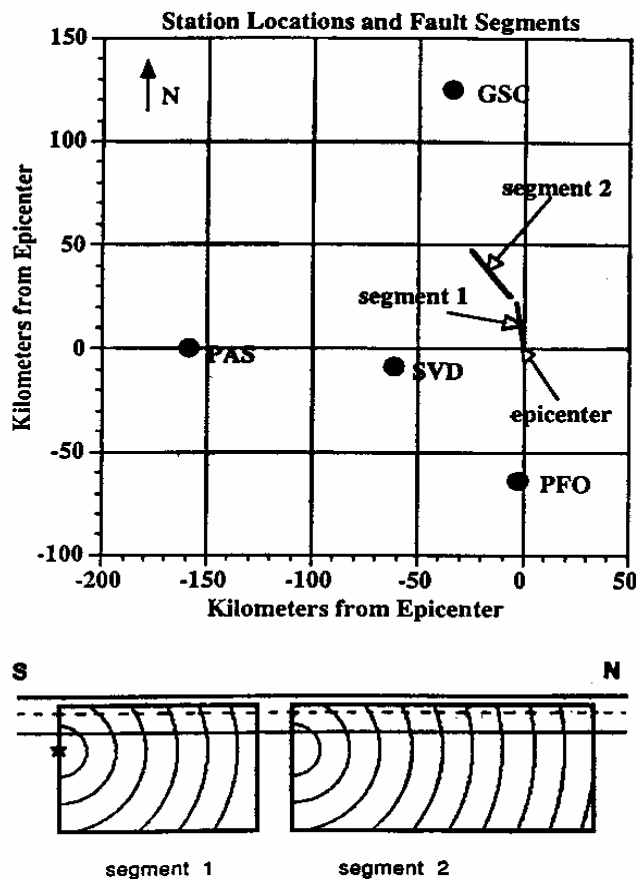


Figure 4. Simplified rupture model of the Landers earthquake

4a. Stations GSC and PFO recorded the 3 components of motion (Z, NS, EW). On which component is mainly recorded the Love waves produced by the earthquake?

The figure 5 shows numerical simulations performed with crustal models 1 and 2 for a simple mostly Haskell-type rupture history. The rupture velocity is 3km/s. Note the fact that the EW motion is very sensitive to the presence of the low velocity layer at GSC while it is almost insensitive at PFO.

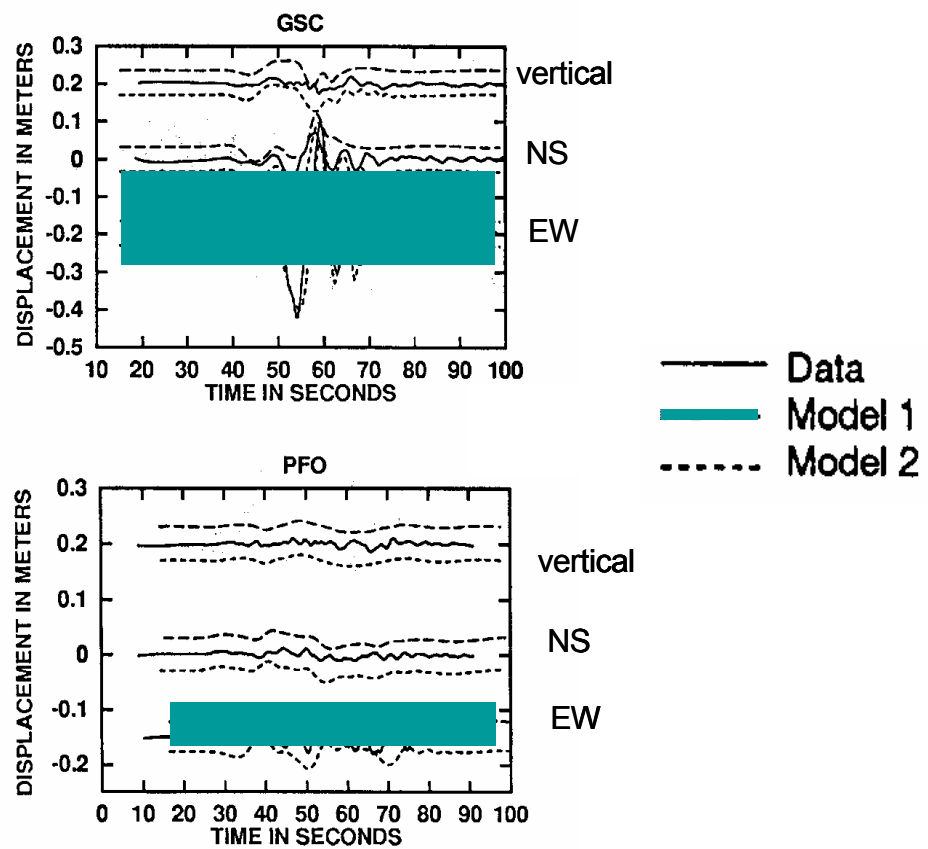


Figure 5. Comparison of observation and numerical simulations for the two crustal models of table 1 and the rupture model of Figure 4.

4b. How can you interpret this fact?

4c. Discuss the importance of the fact that the rupture reaches the surface in terms of strong ground motion prediction.

Theoretical Seismology Exam.
2005-2006. M. Campillo and F. Cotton.
3 hours. Lectures notes accepted.

Part 1

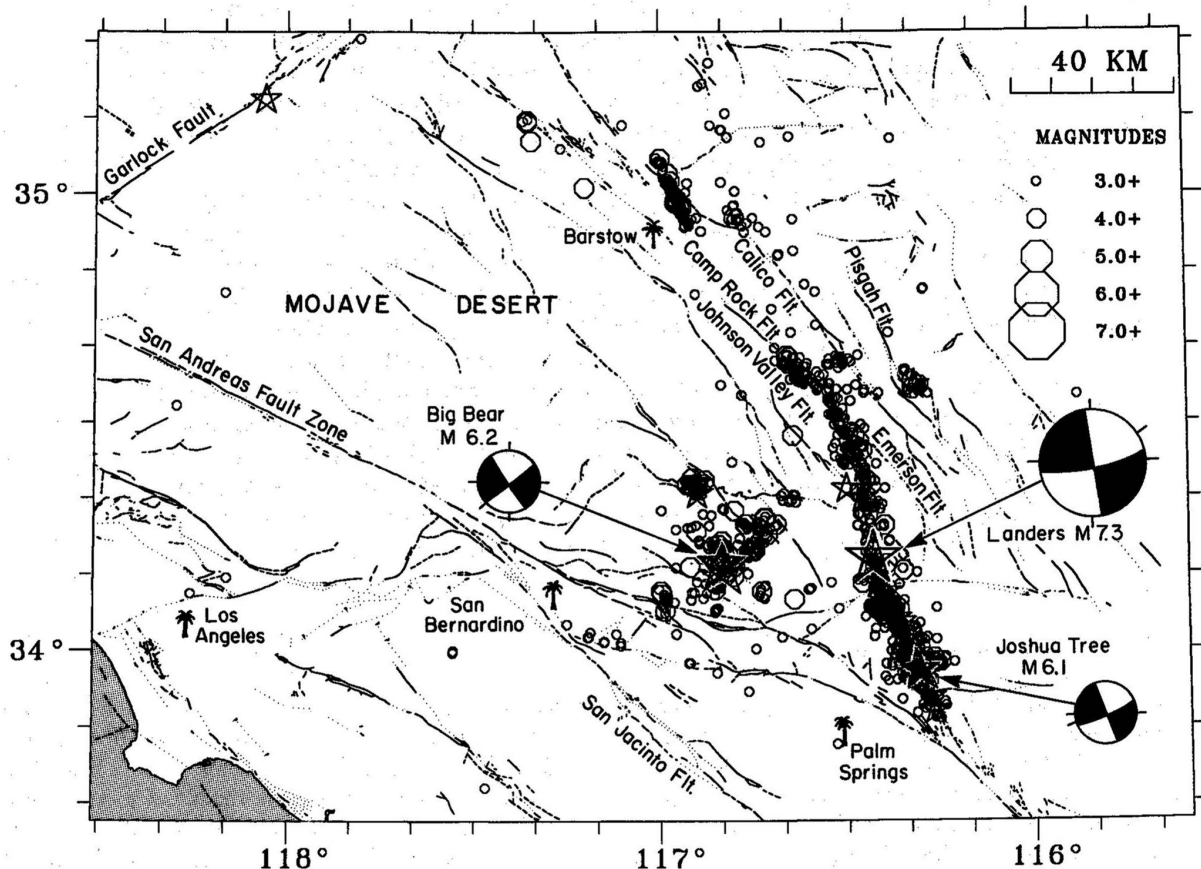


Figure 1. Map of southern California including the eastern California shear zone (Dokka and Travis, 1990), showing major faults from Jennings (1975), and the locations and first-motion focal mechanisms of the 1992 M_w 6.1 Joshua Tree, M_w 7.3 Landers, and M_w 6.2 Big Bear earthquakes and aftershocks of $M \geq 3$. Aftershocks of $M \geq 5$ are shown as stars. Palm trees indicate locations of cities.

Figure 1 shows the focal mechanism of the Landers ($M_w=7.3$) and Joshua Tree ($M_w=6.1$) earthquakes and their aftershocks distributions. Stars indicated the epicentres of the major events.

- 1a. Calculate the Seismic Moment of the Landers and Joshua Tree earthquakes
- 1b. Are these earthquakes strike slip, reverse or normal fault mechanism ?
- 1c. Without any calculation give an estimation of the length and mean slip of the Landers earthquake
- 1d. How many earthquakes of magnitude equal or more than 7.3 do we observe in the world each year ?

Part 2

Model 1
Table 1: Layered Crustal Structure in Southern California

Depth (km)	V _P (km/s)	V _S (km/s)	Density (kg/m ³)	Q _P	Q _S
0.0	5.50	3.20	2800	500	500
4.0	6.30	3.65	2900	500	500
26.0	6.80	3.90	3100	500	500
32.0	8.20	4.70	3200	500	500

Model 2

Depth . km	V _P . km/s	V _S . km/s	Density . Mg/m ³	Q _P	Q _S
0.0	4.1	2.3	2.5	300	300
2.0	5.5	3.2	2.8	500	500
4.0	6.3	3.65	2.9	500	500
26.0	6.8	3.9	3.1	500	500
32.0	8.2	4.7	3.2	500	500

Table 1 presents two falt layers models found in the literature for the crustal structure in southern California. They differ by the presence of a shallow low velocity layer in model 2. We focus in this part on the propagation effects associated with this layer. To simplify we limit our analysis to the case of Love wave. At the first order let consider a single layer over a half space having the properties of the second layer (the case which was treated in the course).

Let consider the harmonic case at frequency f . We consider a plane wave propagating in the shallow layer and contributing to the Love wave. Let us call i the angle of incidence of the plane wave with respect to vertical.

- 2a- Define the phase velocity C in terms of i and the shear wave velocity V_S
- 2b- Give the range of i for which the plane wave can be associated with a Love wave. Identify the lower limit angle and give its numerical value.
- 2c- Demonstrate that a source far below the layer cannot produce a Love wave
- 2d- Explain why the presence of inhomogeneities in the shallow layer can result in the observation of Love waves. In the case when the inhomogeneity consists of a small variation of shear velocity in a known limited volume, does the amplitude of Love wave give an indication on the amplitude of the velocity variation ?
- 2e- We consider again an homogeneous layer over a half space. We remind here the dispersion relation established in the course:

$$\mu(1 - \frac{C^2}{\beta^2})^{1/2} - \mu'(\frac{C^2}{\beta'^2}) - 1)^{1/2} \tan(kh(\frac{C^2}{\beta'^2}) - 1)^{1/2}) = 0$$

Identify and give the values of the parameters you know in the present example.

- 2f Give the limit value of the frequency and the phase velocity associated with the limit $i \rightarrow i_c$ where i_c is the critical angle.

- 2h Same question for $i \rightarrow \frac{\pi}{2}$

Part 3. Directivity effect and slip distribution

Source time function information contained in seismic signals is obscured by propagation and recording effects. To isolate the farfield source time function from propagation and instruments effects, one can deconvolve surface waves (or body waves) of a large event from the surface waves (or body waves) of a moderate-size event. The small event must be near the mainshock and have a similar depth and focal mechanism. An event satisfying these criteria is called an empirical Green Function (EGF) as it constitutes an approximate point source impulse response for a given moment tensor.

Such a deconvolution has been applied by Velasco et al. (1994). The large event is the Landers ($M_w=7.3$) earthquake. The small event (EGF) is the Joshua Tree ($M_w=6.1$) earthquake.

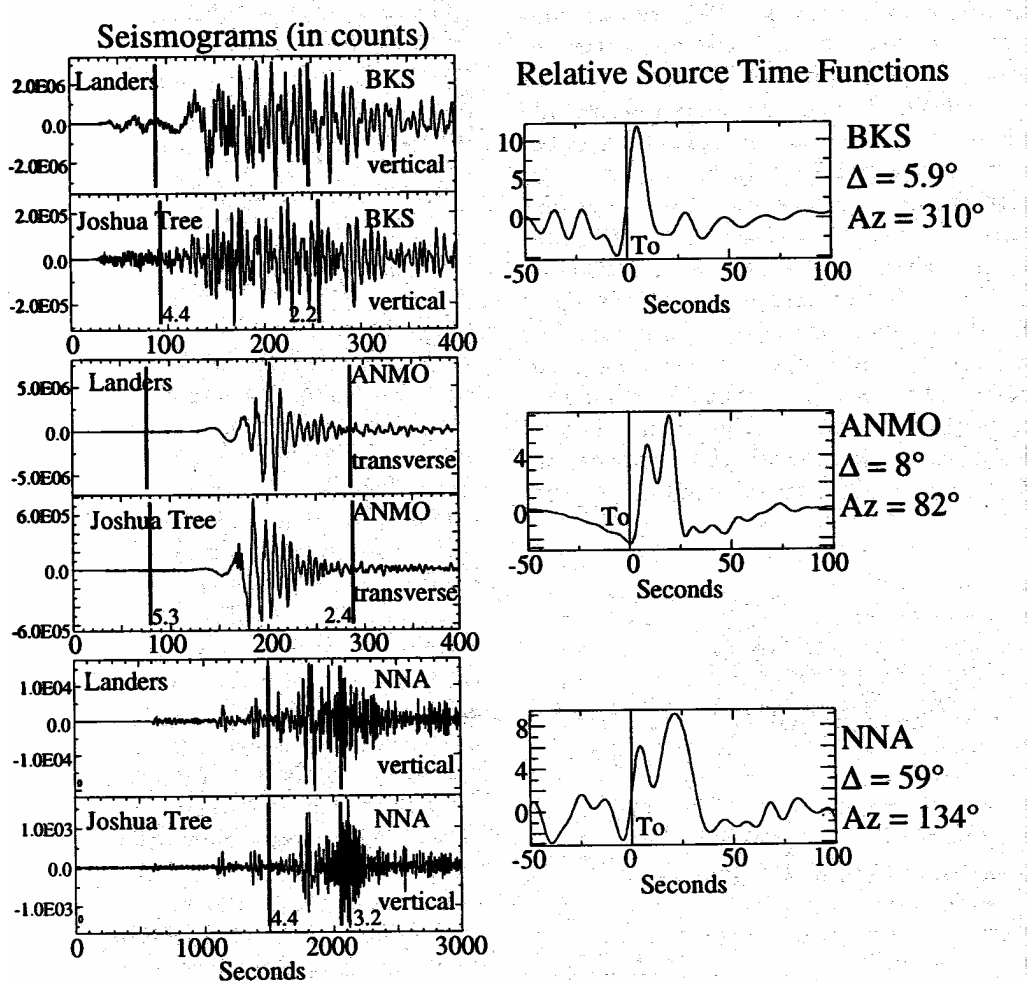


Figure 2. Example of source time function extraction for the deconvolution of surface waves recorded at ANMO, NNA and BKS. Each surface-wave arrival is group velocity windowed (vertical lines in seismogram window). The Joshua Tree ($M_w = 6.2$) earthquake recordings are deconvolved from the Landers ($M_w = 7.3$) earthquake recordings. Each deconvolution gives a relative source time function at each station for the Landers earthquake (right).

The figure 2 shows some source time function extraction $f(t)$ for the deconvolution of surface waves for some teleseismic stations. The station BKS is located north of the Landers earthquake, ANMO is located east of the Landers earthquake (perpendicular to the fault) and NMA located south of the earthquakes.

These source time functions show two pulses for the NMA and ANMO stations and one pulse only for the BKS station. The duration of the source function is larger for the NMA station than for the ANMO station. Velasco et al. explain these complex source times function by directivity effects and by the fact that the earthquake is dominated by two subevents (two regions of high slip separated by a region of lower slip).

In this analysis δt is the measured time difference observed on a station between the onset of the rupture (hypocenter) and the time arrival of the second pulse (second subevent), t_0 is the real time separation between the onset of the rupture and the second subevent and Δ is the distance between the onset of the rupture (hypocenter) and the second subevent.

$$3a. \text{ Show that } \delta t = t_0 - \Gamma \Delta \quad \text{with } \Gamma = \frac{\cos \theta}{c}$$

Γ is a directivity parameter where θ is the azimuth of the station relative to the azimuth of a line connecting the spacial offset between the features and c is the wave velocity which is assumed to be equal to 3.8 km/sec

δt is investigated systematically for stations located at different azimuth from the fault (Figure 3). The preferred fault strike (355°) corresponds to the direction producing the best linear correlation coefficient for (1).

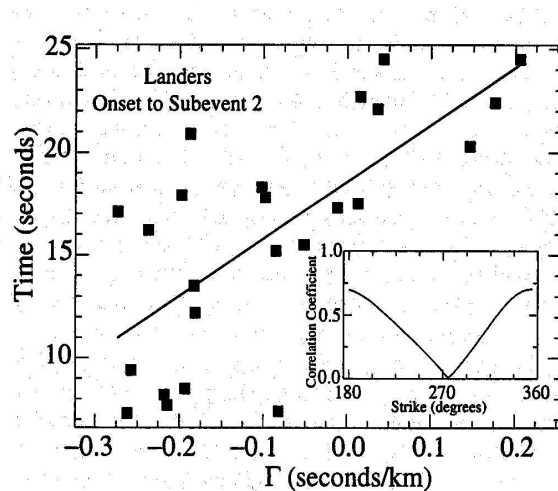


Figure 3 . Directivity analysis of the second subevent relative to the onset of motion of the Landers earthquake. The inset shows the variation of the corresponding linear correlation coefficient as a function of azimuth. The maximum value occurs at a strike of 335° , which is the case shown. Squares correspond to individual observations, the best fitting line is indicated by the solid line.

3b. Which is the distance Δ between the rupture onset and the second subevent ?

3c. Which is the rupture velocity between the onset and the second sub-event ?

We now assume that the entire rupture propagates with constant rupture velocity and that the slip function on each point of the fault is a step function $dD(x,t)/dt=\delta(t)$ where $D(x,t)$ is the slip, x the distance along the strike direction en t the time. $\delta(t)$ represent the dirac function.

The moment rate function is then equal to $\dot{m}(x, t) = m(x) \otimes \delta\left(t - \frac{x}{v_R}\right)$

with $m(x) = \mu W S(x)$ μ is the shear modulus, W the width of the fault and $S(x)$ the slip on the fault along the strike direction.

The source time function $f(t)$ observed at station ANMO perpendicular to the fault can then be written

$$f(t) = \frac{\left(\int_{-\infty}^{\infty} m(x, t) dx\right)}{m_0_{egf}}$$
 where m_0_{egf} is the seismic moment of the Joshua Tree earthquake used as EGF in the deconvolution.

3d. Using the following relationship $\delta(ax + b)) = \frac{1}{|a|} \delta\left(x + \frac{b}{a}\right)$ show that

$$f(t) = \frac{(v_R m(tv_R))}{m_0_{egf}}$$

3e. Using the $f(t)$ observed at the station ANMO deduce the slip profile of the Landers earthquake along the fault.

Part 4. Interpretation of strong motions

A simplified model of the Landers rupture with 2 linear segments is presented in Figure 4. The rupture reaches the upper low velocity layer (dashed line). On each segment the rupture develops in a manner similar to the Haskell model.

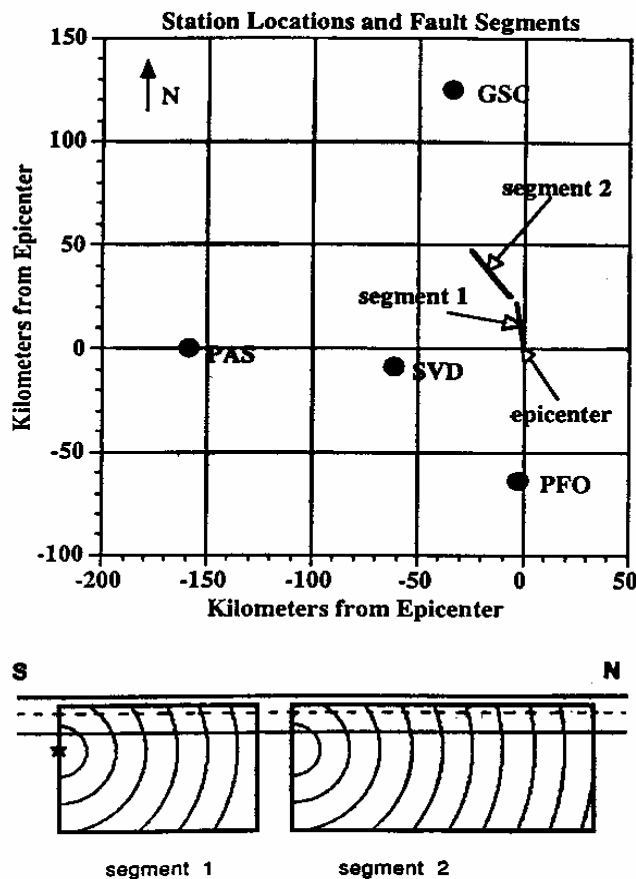


Figure 4. Simplified rupture model of the Landers earthquake

4a. Stations GSC and PFO recorded the 3 components of motion (Z, NS, EW). On which component is mainly recorded the Love waves produced by the earthquake?

The figure 5 shows numerical simulations performed with crustal models 1 and 2 for a simple mostly Haskell-type rupture history. The rupture velocity is 3km/s. Note the fact that the EW motion is very sensitive to the presence of the low velocity layer at GSC while it is almost insensitive at PFO.

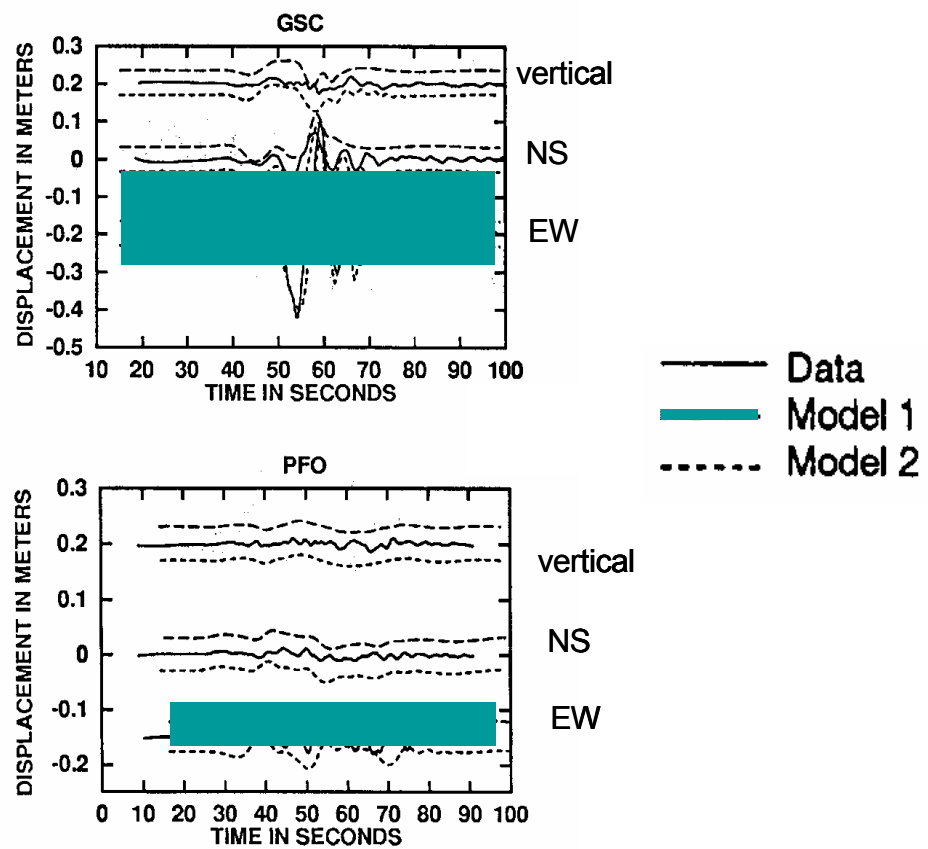


Figure 5. Comparison of observation and numerical simulations for the two crustal models of table 1 and the rupture model of Figure 4.

4b. How can you interpret this fact?

4c. Discuss the importance of the fact that the rupture reaches the surface in terms of strong ground motion prediction.